Arkadiusz MIASKOWSKI[1], Andrzej KRAWCZYK[2,3]

University of Life Sciences in Lublin (1), Politechnika Częstochowska (2), Wojskowy Instytut Higieny I Epidemiologii (3)

Magnetic Fluid Hyperthermia for Cancer Therapy

Abstract. *The aim of the paper is to show basic ideas of magnetic fluid hyperthermia treatment with regard to power losses which occur during heating with alternating magnetic field. A special attention has been paid to dielectric, hysteresis and relaxation mechanism losses and their contribution to total power losses. A numerical analysis has been done with regard to a simplified female breast phantom and its dielectric parameters.*

Streszczenie. *W artykule przedstawiono fizyczne podstawy hipertermii cieczy magnetycznej ze szczególnym uwzględnieniem strat mocy, jakie zachodzą podczas grzania zmiennym polem magnetycznym tkanek ludzkich połączonych z cieczą magnetyczną. I tak, zaprezentowano straty wiroprądowe, histerezowe i relaksacyjne, a następnie dokonano numerycznej analizy rozkładu gęstości mocy w zastosowaniu do parametrów dielektrycznych tkanek gruczołu piersiowego.* ***(Zastosowanie hipertermii cieczy magnetycznej w terapii antynowotworowej)****.*

Keywords: magnetic fluid hyperthermia, Finite Element Method, computer simulation.
Słowa kluczowe: hipertermia cieczy magnetycznej, metoda elementów skończonych, symulacja komputerowa.

Introduction

Hyperthermia is a method of treating cancer by preferentially heating the tumor. Generally speaking, it involves reaching and maintaining for several minutes a temperature of 42 to 48 ^{0}C in the tissues [1]. There are three main approaches to hyperthermia treatments i.e. whole-body hyperthermia, regional and localized hyperthermia. The whole-body hyperthermia raises the temperature of the entire body to nearly 42^{0}C, and it is often uncomfortable for the patients due to high temperature gradients. Besides, the tumors may not reach sufficiently high temperatures. Regional hyperthermia attempts to heat moderately large volumes, such as thorax or pelvis including the cancerous region as well as surrounding healthy tissues. The remainder of the body is kept as close to normal temperature as possible. Localized hyperthermia heats mainly the tumors and it is mostly used for superficial tumors [2].

The above three types of hyperthermia are connected with serious engineering challenges i.e. to provide uniform heating throughout the target volume to ensure that all cancerous tissues reach therapeutic temperature and achieve adequate temperature in deep tumors without overheating the body surface. Recently, magnetic fluid hyperthermia has offered some attractive possibilities to overcome these engineering problems remaining in hyperthermia [3].

Magnetic fluid hyperthermia, which is the combination of inductive applicator and magnetic fluid (nanoparticles) injected into cancerous tissues, has attracted much attention because of their considerable heating effects in time-varying magnetic field. It can increase the temperature in tumors to 43 − 48^{0}C, and therefore leads to apoptosis (see Fig. 1).

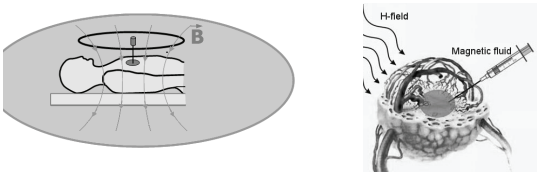

Fig. 1. Idea of magnetic fluid hyperthermia (left); feeding magnetic fluid to tumor or cancer (right)

From Fig. 1 one can see that magnetic fluid hyperthermia can be divided into three steps:
1. Feeding magnetic fluid to tumor or cancer;
2. Applying external EMF of hundreds of kHz;
3. Tumor or cancer is destroyed (apoptosis).

It emerges from this that one of the focal points that should be clarified for magnetic fluid hyperthermia is how to generate a therapeutical temperature of at least 43^{0}C inside the tumor.

Magnetic Loss Processes

Magnetic losses in an alternating magnetic field responsible for power dissipation e.g. to be utilized for heating arise from:
1. Hysteresis;
2. Néel or Browian relaxation.

Hysteresis losses may be determined in a well known manner by integrating the area of hysteresis loops, a measure of energy dissipated per cycle of magnetization. It depends on the field amplitude, the magnetic prehistory as well as the magnetic particle size domain [4]. On the other hand, the hysteresis losses can be estimated as it has been proposed in [5], where heat capacity Q generated by magnetite can be calculated as follows:

$$Q = k_m f D_w B^2 \quad \left[\frac{W}{ml}\right] \tag{1}$$

where: • km= 2.4 -10^{-3}[W/Hz/(mgFe/ml)/T^2/ml], f - exciting frequency of applied field [Hz], B - external magnetic field [T], D_w- weight density of magnetic fluid [mgFe/ml].

As for relaxation mechanisms of ferrofluids there are two physical processes responsible for the power dissipation - Néel and Browian relaxations [6]. Néel relaxation is connected with the fluctuation of magnetic moment direction across an anisotropy barrier and the characteristic relaxation time τ_N a nanoparticle system is given by the ratio of the anisotropy energy KV to the thermal energy kT as follows [7]:

$$\tau_N = \tau_0 \exp\left[KV/(kT)\right] \tag{2}$$

where ($\tau_0 \approx 10^{-9}$s). For a characteristic time of measurements τ_m a critical particle volume V_c may be defined by $\tau_N(V_c) = \tau_m$ (see Fig. 2 - the arrow indicates the direction of magnetization).

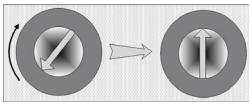

Fig. 2. Néel relaxation, direction of magnetization rotates in core.

In the case of the second relaxation mechanism, the time associated with the rotation diffusion is the Brownian relaxation time τ_B where [8]:

$$\tau_B = 4\pi\eta r_h^3/(kT) \tag{3}$$

r_h is the hydrodynamic radius which due to particle coating may be essentially larger than the radius of the magnetic particle core (see Fig. 3 - the arrow indicates the direction of magnetization).

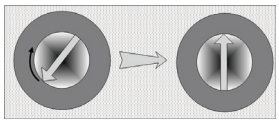

Fig. 3. Brownian relaxation, entire particle rotates in fluid.

In general, the faster of the relaxation mechanisms is dominant and an effective relaxation time may be defined by

$$\tau_{eff} = \frac{\tau_N \tau_B}{\tau_N + \tau_B} \tag{4}$$

Taking into account the frequency dependence of relaxation of the particle ensemble may be investigated experimentally by measuring the complex susceptibility. The imaginary part $\chi''(f)$, which is related to magnetic losses, can be expressed as:

$$\chi''(f) = \chi_0 \phi/(1+\phi^2) \tag{5}$$

where $\phi = f\phi_{N,B}$, $\chi_0 = \mu_0 M_s^2 V/(kT)$ and M_s is saturation magnetization. Within the validity of linear response theory the loss power density p_χ is related to $\chi''(f)$ as follows:

$$p_\chi(f,H) = \mu_0 \pi \chi''(f) H^2 f \tag{6}$$

The above formulas (1) and (6) have been used in a numerical solver based on Finite Element Method (FEM) as described below.

Numerical solver

In order to investigate the combination of the overheating effect of magnetic nanoparticles and the eddy current one, the authors have prepared the FEM solver based on FEniCS project [8] as follows. Taking into account low conductivity of human tissues and low frequency of electromagnetic field the considered problem has been divided into a few steps. Firstly, the current density (J_c) in the torus shape coil has been calculated. Secondly, describing magnetic field by magnetic vector potential A and knowing that $\nabla \times A = B$ a partially differential equation for magnetic field has been formulated:

$$\nabla \cdot \nabla A = -\mu_0 J_c \tag{7}$$

Next, using electric scalar potential (φ) the eddy current problem in human tissues has been defined as follows:

$$\nabla \cdot \sigma \nabla \varphi = -\nabla \cdot \left(\sigma \frac{\partial A}{\partial t} \right) \tag{8}$$

where σ is the conductivity of tissues. Then current density vector can be expressed as the sum of two components:

$$J = -\sigma \nabla \varphi - \sigma \frac{dA}{dt} \tag{9}$$

Power density (p_e) produced by the eddy currents can be expressed as:

$$p_e = \frac{J^2}{\sigma} \tag{10}$$

Finally, in order to include in our model both, the hysteresis losses and the power density from eddy currents, one can present the total power density as follows:

$$p_{tot} = p_e + p_Q = \frac{J^2}{\sigma} + k_m D_w f B^2 \tag{11}$$

On the other hand, the total power density is the product of both the power density from eddy currents and power dissipation from magnetic nanoparticles. Therefore, one can write:

$$p_{tot} = p_e + p_\chi = \frac{J^2}{\sigma} + \mu_0 \pi \chi'' f H^2 \tag{12}$$

The above formulas for total power density (p_{tot}) have been numerically evaluated and the obtained results have been compared.

The phantom model and results

The methodology described above has been applied to calculate the power density distribution with regard to the female breast phantom dielectric properties. Three different layers i.e. the layer of skin, breast fat and muscle (equivalent to cancerous tissue) have been distinguished in the phantom, as it is shown in Fig.4 [9].

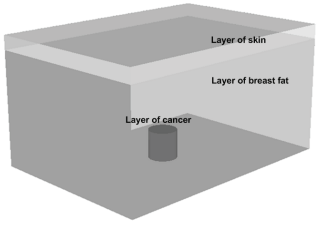

Fig. 4. The CAD model of female breast and its layers.

The dielectric properties of the phantom were approximated for the frequency of 150 kHz with the use of the 4-Cole-Cole model and parameters taken from Gabriel [10] (see Tab. 1).

Table 1. Dielectric properties of the phantom

No.	Layer name	Conductivity [S/m]
1	Skin	0.089
2	Breast FAT	0.025
3	Muscle/Tumor	0.37

As the excitation the 5-turn torus coil flowing current with amplitude of I = 400A has been used. The coil has been placed about 3 cm above the layer of skin of the phantom. The lines of picture show magnetic field generated by the coil, as it is shown in Fig. 5.

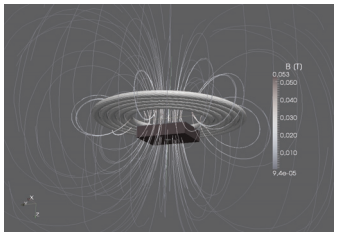

Fig. 5. The complete simulation model consists of the coil and the simplified breast model. Lines of the picture show magnetic field generated by the coil.

In Fig.6 power density distribution from eddy currents in logarithmic scale can be seen (see formula (10)).

Fig. 6. Distribution of power density p_e.

To evaluate the relaxation mechanism and its contribution in power dissipation in the model the total power density has been calculated using formula (12). One should realize that $\tau_B >> \tau_N$ and therefore τ_B can be neglected ($\tau_B = 10^3 \tau_N$). Moreover, according to [3] $\chi'' \approx$ [5, 10, 15] at frequency 150 kHz and in our case χ = 10 has been used in calculations. In Fig.7 is shown power density distribution form the eddy currents (p_e) and from relaxation mechanism (p_χ)

Fig. 7. Distribution of the total power density $p_e + p_\chi$.

In order to calculate the hysteresis losses using formula (1) the weight density of magnetic fluid, D_w = 10 mgFe/ml, has been used, which is equivalent to, for example, Resovit produced by Meito Sangyo Co. from Japan. Finally, in Fig.8 the total power density distribution from the eddy currents (p_e) and from hysteresis can be seen (p_Q).

Fig. 8. Distribution of the total power density $p_e + p_Q$.

In Table 2 the maximum values of power density for three considered cases have been gathered. One can conclude that the maximum values of p_e have occurred in the skin layer but they are negligible when compared with p_Q and $p\chi$, which occurred in the cancer layer. Moreover, the values of p_Q and $p\chi$ are very close. It emerges from this that the experimentally developed formula (1) is proper.

Table 2. Maximum values of power densities

pe[W/m3]	p_Q[W/m3]	p_χ[W/m3]
108e3	8.61e8	8.65e8

Conclusions

The power density in the cancer layer is about 8000 times higher with magnetic fluid than without it. That means that eddy currents effects are completely negligible regarding the heating of the injected magnetic fluid. At this point the authors would like to underline that the terminus inductive heating occasionally used for magnetic heating in biomedicine is misleading, as it has been shown in this paper.

Eddy currents are important when talking about inductive heating. The maximum power density values in the body are determined by the size of body, and so is the distance between the applicator and the skin. Nevertheless, the knowledge of p_e plays an important role when skin overheating is taken into consideration.

In our simplified model we have not considered the presence of blood flow and tissue perfusion, both of which are dominant sources of tissue cooling, and both of which vary actively as the tissue is heated, but the proposed approach offers a very simple methodology of energy deposition.

REFERENCES

[1] Kurgan E., Gas P., Estimation of Temperature Distribution Inside Tissues in External RF Hyperthermia, Electrical Review (Przegląd Elektrotechniczny), 12, 2010, 100-102.

[2] Furse C., Christensen D.A., Durney C.H.: Basic introduction to bioelectromagnetics, CRC Press, Second edition, 2008.

[3] Jordan A. et al.: Presentation of a new magnetic field therapy system for the treatment of human solid tumors with magnetic fluid hyperthermia, Journal of Magnetism and Magnetic Materials, Vol. 225, pp. 118-126, 2001.

[4] Herget R., Dutz S., Muller R,. Zeisberger M.: Magnetic particle hyperthermia: nanoparticle magnetism and materials development for cancer therapy, Journal of Physics: Condensed Matter, Vol. 18, pp. S2919-S2934, 2006.

[5] Yamada S., et al.: Detection of Magnetic Fluid Volume Density with a GRM Sensor, Journal of Magnetic Soc. Jpn., Vol. 31, pp. 44-47, 2007.

[6] Rosenweig R.E.: Heating magnetic fluid with alternating magnetic field, Journal of Magnetism and Magnetic Materials, Vol. 252, pp. 370-374, 2002.

[7] Fannin P.C.: Magnetic spectroscopy as an aide in understanding magnetic fluids, Journal of Magnetism and Magnetic Materials, Vol. 252, pp. 59-64, 2002.

[8] Logg A. and Wells G.N.: DOLFIN: Automated finite element computing, ACM Transactions on Mathematical Software, 37(2), Article 20, 28 pages, 2010.

[9] Miaskowski A., Sawicki B., Krawczyk A., Yamada S.: The application of magnetic fluid hyperthermia to breast cancer treatment, Electrical Review (Przegląd Elektrotechniczny), 12 , 2010 pp. 99-101.

[10] Gabriel C., Gabriel S. and Corthout E.: The dielectric properties of biological tissues: III. Parametric models for the dielectric spectrum of tissues, Physics in Medicine and Biology, Vol. 41, pp. 2271-2294 1996.

Authors: *Ph.D. Arkadiusz Miaskowski, University of Life Sciences in Lublin, Department of Applied Mathematics and Computer Science, Akademicka 13, 20-950 Lublin, Poland, email: arek.miaskowski@up.lublin.pl, Prof. Andrzej Krawczyk, Czestochowa University of Technology, ul. Armii Krajowej 17, 42-200 Czestochowa, Military Institute of Hygiene and Epidemiology, Kozielska 4, 01-163 Warszawa, Poland, email: a.krawczyk@el.pcz.czest.pl*